



Uncorrected satellite derived shoreline data assimilation in equilibrium modelling

Georgios AZORAKOS ¹, Bruno CASTELLE ¹,
Vincent MARIEU ¹, Déborah IDIER ²

1. Université de Bordeaux, CNRS, Bordeaux INP, EPOC, UMR 5805, Allée Geoffroy Saint Hilaire, Pessac, 33615, Nouvelle Aquitaine, France.

georgios.azorakos@u-bordeaux.fr; bruno.castelle@u-bordeaux.fr;

vincent.marieu@u-bordeaux.fr

2. BRGM, 3 Av. Claude Guillemin, Orléans, 45100, Centre, Val de Loire, France.

d.idier@brgm.fr

Abstract:

In the present work, a state-of-the-art equilibrium shoreline model was calibrated using alongshore averaged uncorrected satellite derived shoreline (SDS) data on a high-energy meso-macrotidal gently sloping beach, with error exceeding 30 m. The model was forced by the freely available ERA5 wave hindcast and its performance was addressed using in-situ surveys. A simulated annealing non-linear optimization algorithm was used to find the best fit model parameters, assuming no a priori knowledge of the simulated coastal environment. Finally, a data assimilation routine was applied to investigate the temporal variability of the model free parameters and their correlation with the environmental conditions.

To the authors knowledge this study is one of the first applications of uncorrected SDS for model calibration in a meso- macrotidal environment. Despite the large uncertainties of the SDS data, the calibrated model has an error slightly above 10 m and manages to reproduce approximately 75% of the observed shoreline variability. The preliminary results of the model free parameters time evolution obtained through assimilation shows interannual patterns potentially linked with interannual winter wave height variability. Understanding the correlation between environmental conditions and parameter variability would open new perspectives for shoreline evolution predictions.

Keywords:

Shoreline modelling, Satellite data, Calibration, Data assimilation.

1. Introduction

Understanding and predicting sandy shoreline evolution over the next decades is key to effective conservation and management of coastal ecosystems. Although skilful and efficient on cross-shore transport dominated sites, reduced complexity equilibrium shoreline models strongly rely on data spanning over several years for the calibration of

Thème 6 – Risques côtiers

the free parameters and are thus restricted to a few well monitored sites in the world (SPLINTER *et al.*, 2014).

Publicly available satellite imagery has cradled a new approach in remote sensing providing long term high temporal resolution shoreline data with global coverage (VOS *et al.*, 2019). SDS positions however come with uncertainties that challenge their usability especially in meso- macrotidal, high energetic coasts, where horizontal position errors can exceed 30 m (CASTELLE *et al.*, 2021).

In the present work we explore the challenges and opportunities stemming from the availability of optical satellite imagery and their use in equilibrium shoreline modelling. First, we assess the applicability of uncorrected SDS in model calibration at the meso-macrotidal high energetic beach of Truc-Vert in southwest of France, assuming no a priori knowledge of the site. Successively, a data assimilation routine is used to investigate the links between the model's free parameter evolution and environmental conditions.

2. Study site

Truc Vert is a high energy meso-macrotidal double barred open beach backed by high (~20-25 m above Mean Sea Level, AMSL) and wide (~250 m) coastal dunes (see Figure 1). Tide is semi-diurnal with an annual mean spring tidal range of ~ 3.7 m and largest tidal range of ~ 5 m. The wave climate is seasonally modulated with monthly average significant wave height $\overline{H_s}$ and peak wave period $\overline{T_p}$ ranging from 1.11 m and 9 s in July, with a dominant west-northwest direction, to 2.4 m and 12.8 s in January with a dominant west direction (CASTELLE *et al.*, 2020). The sediment composition primarily consists of medium quartz sand, with a median diameter of $d_{50} \sim 350 \mu\text{m}$. The beach sediment displays substantial variability ranging from 200 μm to 700 μm , associated with a wide range of bedforms such as bar/rip channels, megacusps, cusps, and megaripples (GALLAGHER *et al.*, 2011). The outer bar is subtidal and modally crescentic, while the inner bar, situated in the intertidal zone, is mostly classified as a transverse bar and rip and during the summer months tends to transition into a low tide terrace. The average spacing between rip channels is approximately 400 m for the inner bar and 700 m for the outer bar, although these values can vary considerably over space and time. The presence of rip channels incising the inner bar leads to significant alongshore variations in beach morphology, with pronounced megacusp embayments (Figure 1) in the alignment of the rip channels typically evolving on seasonal timescales. The outer bar on the other hand, can drive larger scale beach variability during severe storms which can persist for several years (CASTELLE *et al.*, 2020).

3. Methodology

A hybrid two-step approach is adopted here, aiming to assess the usability of uncorrected SDS data for shoreline model calibration and further explore the links between temporally evolving model parameters and environmental conditions through data assimilation. A

timeseries of uncorrected alongshore averaged SDS data \overline{W}_s was computed from instantaneous waterlines extracted over a 4-km alongshore window at Truc Vert beach (see Figure 1), using the freely available python toolkit CoastSat (VOS *et al.*, 2019). A georeferencing error of maximum 10 m has been applied for the extraction of the instantaneous waterlines while no correction considering the water level during the satellite fly over time has been applied. The \overline{W}_s dataset was compared by CASTELLE *et al.*, (2021) to the alongshore averaged +1.5 m AMSL shoreline proxy \overline{S}_{IS} derived from in-situ RTK DGPS surveys, and showed a RMSE exceeding 30 m. For a detailed description of the two shoreline datasets (in-situ surveyed and satellite derived) the reader is referred to the works of CASTELLE *et al.*, (2020, 2021).

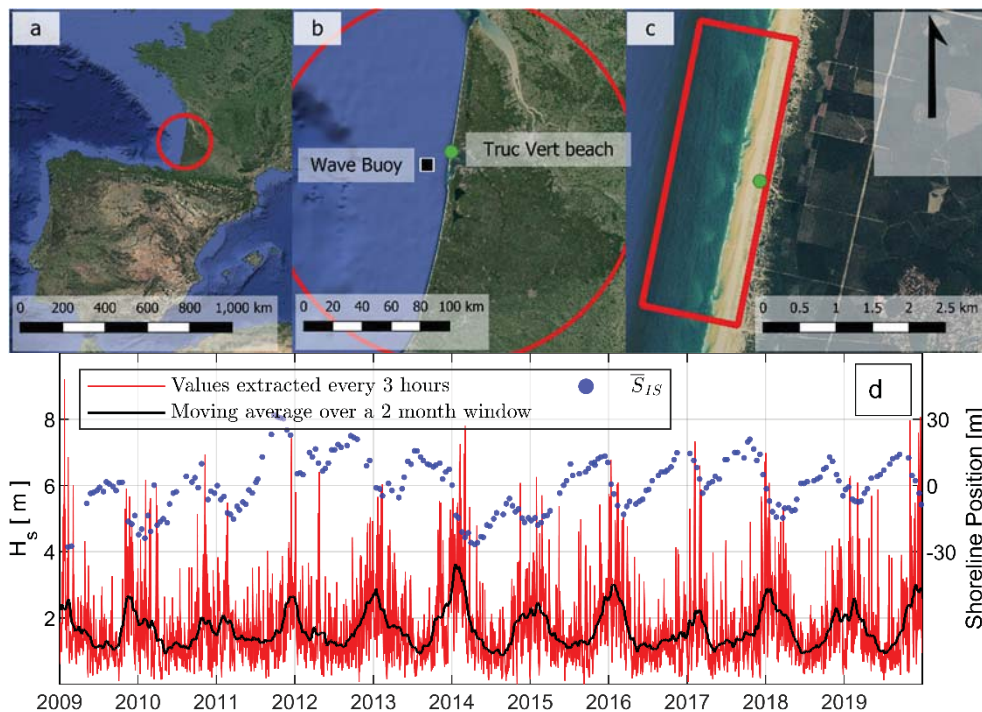


Figure 1. (a) Overview of the area (b) Location map of Truc Vert beach, southwest France indicating the position of the CANDHIS wave buoy (Cap Ferret wave buoy 03302). (c) Survey zone at Truc Vert beach. (d) Offshore wave height extracted at the location of the buoy for the considered period. The alongshore averaged in-situ shoreline is depicted in blue dots on the right axis.

The state-of-the-art equilibrium shoreline model, proposed by DAVIDSON *et al.*, (2013) was calibrated using the \overline{W}_s dataset and validated against the \overline{S}_{IS} dataset. A simulated annealing non-linear optimization algorithm proposed by BERTSIMAS & TSITSIKLIS (1993) was used to find the best fit model parameters, assuming no a priori knowledge of the site. To ensure the no a priori knowledge assumption, the range of the investigated model free parameters extended beyond the limits found in the literature. Finally, the data

Thème 6 – Risques côtiers

assimilation routine implemented by IBACETA *et al.*, (2020) was applied to investigate the temporal variability of the model free parameters and their correlation with the environmental conditions. A twenty-year dataset of alongshore averaged uncorrected SDS was assimilated in the model which was forced by the freely available ERA5 wave dataset described in HERSBACH *et al.*, (2020). The ERA5 wave timeseries has been extracted from the grid point closest to the buoy coordinates (see Figure 1) and shoaled using the LARSON *et al.*, (2010) formula to account for the offshore wave direction.

The shoreline displacement in the model of DAVIDSON *et al.*, (2013), is defined as a function of the nearshore wave power and a disequilibrium state of the beach, with the rate of shoreline change being defined as:

$$\frac{dx}{dt} = c^{\pm} P^{0.5} (\Omega_{eq} - \Omega) \quad (1)$$

The model's forcing term is the product of the incident wave power P (W) computed using linear wave theory, and the model free parameter c^{\pm} representing the response rate of the shoreline with units of velocity per measure of incident wave power. The parameter c^{\pm} is separated into accretion c^{+} when $\Omega_{eq} > \Omega$ and erosion c^{-} when $\Omega_{eq} < \Omega$ components, accounting for the fact that accretion and erosion are observed to evolve at different rates. The formulation of DAVIDSON *et al.*, (2013) included an additional term b , accounting for linear trends stemming from longer term processes that are not explicitly addressed in the model. In the present work this term is disregarded due to the relatively small trend calculated from the SDS data. The term inside the parenthesis in Equation (1) is a disequilibrium term which is based on the premise that shoreline state and morphological change are inter-related. Ω is the dimensionless fall velocity defined as:

$$\Omega = \frac{H_s}{T_p w_s} \quad (2)$$

H_s and T_p are the instantaneous significant wave height and peak wave period respectively and w_s is the terminal fall velocity of the beach's median grain diameter d_{50} calculated using Stoke's law. The time varying equilibrium condition Ω_{eq} is a weighted average of the antecedent dimensionless fall velocity Ω defined as:

$$\Omega_{eq} = \sum_{j=0}^{2\varphi} \Omega_j 10^{-j/\varphi} \left[\sum_{j=0}^{2\varphi} 10^{-j/\varphi} \right]^{-1} \quad (3)$$

where j is the number of days prior to the present and the memory decay φ is a model free parameter indicating the number of days it takes for the weighting to reach 10 %, 1 % and 0.1 % of the instantaneous value at φ , 2φ and 3φ days prior to the present.

4. Model calibration

In Figure 2 the results of the model calibration using the \bar{S}_{IS} and \bar{W}_s datasets are depicted, while the mean values of the calibrated model free parameters are summarized in Table 1. The model has been calibrated over a five-year period and validated against the subsequent six-year period. The choice of the calibration period was made in line with the study of SPLINTER *et al.*, (2014) where they investigated the adequate duration of calibration. The experiment was repeated 10 times to account for the stochastic nature of the simulated annealing algorithm. The results of the experiment are summarized in terms of root mean square error RMSE and coefficient of determination R^2 in the legend of the figure for both the calibration and validation periods. The two datasets used for the calibration and validation of the model are also depicted in the figure. The RMSE and R^2 of the \bar{W}_s dataset compared to the \bar{S}_{IS} is also indicated in the legend.

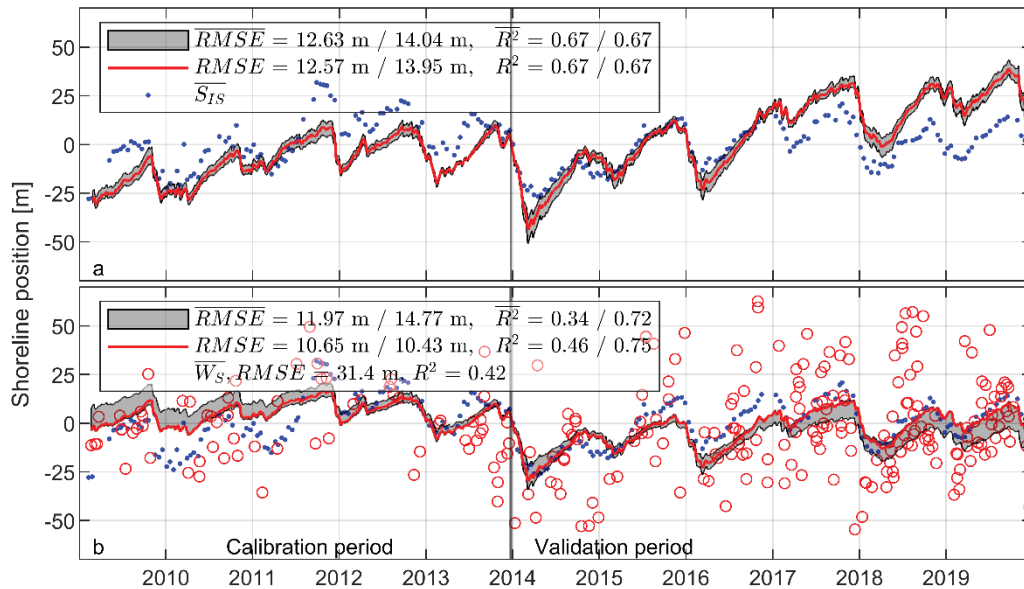


Figure 2. Calibration results using the \bar{S}_{IS} data (panel a) and the \bar{W}_s data (panel b). Model is validated against the \bar{S}_{IS} dataset. Grey area indicates the range of predicted shorelines from an ensemble of 10 simulations, while the red line is the ensemble mean. RMSE and R^2 calculated against the \bar{S}_{IS} data are indicated in the legend for both simulated shorelines as well as for the Satellite Derived shorelines.

The SDS dataset used has a large RMSE and captures a little more than 40% of the shoreline variability observed in the \bar{S}_{IS} dataset. Nonetheless, the calibrated model has an error slightly above 10 m and manages to reproduce 75% of the observed variability. The two datasets (in-situ and satellite derived) when used in model calibration yield very similar values for the model free parameters (see Table 1) and manage to generate a model with very similar skill (see Figure 2). Both datasets when used for calibration yield large ϕ values (see Table 1) associated with coasts like Truc Vert illustrating seasonal

Thème 6 – Risques côtiers

dominated behaviour (SPLINTER *et al.*, 2014; IBACETA *et al.*, 2020). The model calibrated using the \overline{S}_{IS} dataset has a significantly larger accretion rate compared to the one calibrated using \overline{W}_S dataset (see table 1). This is the reason for the erroneous trend forecasted by the model dataset in the validation period, which suggests that the model is sensitive to the period/data used for their calibration.

Table 1. Calibrated model free parameters

Calibration dataset	φ	c^+/c^-
\overline{W}_S	1302	$0.43/0.10 \times 10^{-7}$
\overline{S}_{IS}	1267	$0.70/0.14 \times 10^{-7}$

5. Data assimilation

In Figure 3, preliminary results of the parameter variability investigation are presented. The shoreline change estimates are depicted in the upper panel of the figure together with the shoreline datasets used in the assimilation. The RMSE and R^2 of the two models are calculated against the \overline{S}_{IS} dataset and indicated in the legend. The duration of the four available satellite missions is plotted in colour bars at the bottom, while the revisiting period is indicated in the legend. In the lower panel of the figure the temporally varying memory decay parameter is depicted for the assimilated period. The variability of the model parameters was calculated using the Ensemble Kalman Filter methodology presented in IBACETA *et al.*, (2020). Tracking the variability of the beach memory decay parameter can be challenging as the model has been found relatively insensitive to values of $\varphi > 100$ days (IBACETA *et al.*, 2020), which is why the calibration and data assimilation approach show such large difference in the magnitude of φ .

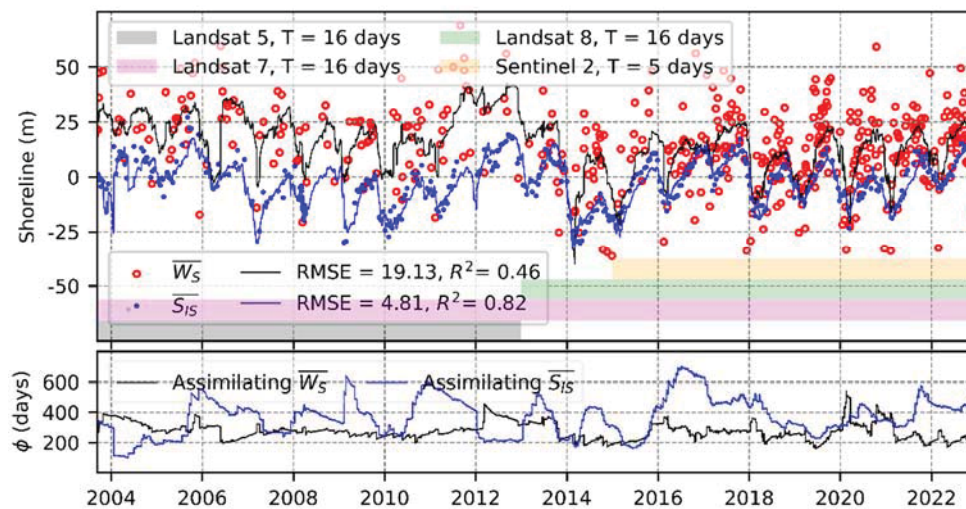


Figure 3. Upper panel: Simulated Shoreline assimilating SDS data (red dots) and in situ data (blue dots) plotted in black and blue lines respectively. The colour bars at the bottom indicate the duration of each satellite mission. Lower panel: Evolution of the beach memory parameter.

Although not directly comparable as the modelling period is different, the model assimilating the in-situ data illustrates a significant improvement compared to the calibration case (see Figure 3). The enhanced model skill is attributed to the non-stationarity in the free parameters enabling the model to adjust based on the prevailing conditions. The time evolving beach memory remains large ($\varphi \simeq 600$ days) during periods with average seasonal behaviour while significantly drops during the more energetic winters like 2013-2014 ($\varphi \simeq 200$ days), similar to the work of IBACETA *et al.*, (2020).

Although the model assimilating the SDS data manages to outperform the assimilated dataset (see Figure 2), the performance is worse compared to the calibration case. In the later stages of the simulation (notably after 2013), the model performance seems to improve as it manages to better reproduce the observed shoreline. This coincides with the emergence of two more satellite missions (Landsat 8 at 2013 and Sentinel 2 at 2015) contributing to the quality of the dataset both in terms of accuracy and observation frequency.

6. Conclusion

The model skill obtained when using uncorrected, noisy SDS data for calibration, is similar to that using accurate field data. This result indicates that the simulated annealing algorithm is capable of finding the optimal solution even when applying a very challenging dataset with large error and seasonal/interannual patterns barely depictable. This finding indicates strong potential for the use of SDS data in cross shore transport dominated sites, even in sites as challenging as Truc Vert (macro tidal and high energetic). The data assimilation study aiming to track the temporal variability in model free parameters is considered to be still at a preliminary stage. Nonetheless some interesting and promising results have been obtained. The temporal variability of the model parameters is pronounced when assimilating the in-situ data. Understanding the correlation between environmental conditions and parameter variability would enable us to explore the potential of non-stationary parameters in model applications for future shoreline predictions.

To the authors' knowledge the current study constitutes one of the first successful applications of uncorrected SDS data for the calibration of an equilibrium shoreline model in a high-energy, meso- macrotidal environment such as Truc Vert. Given that Truc Vert is a challenging site for SDS, the adopted methodology shows potential for global applications at cross-shore transport dominated sites.

7. Acknowledgements

This work was done in the framework of SHORMOSAT project funded by Agence Nationale de la Recherche (Grant ANR-21-CE01-0015) and PSGAR CORALI (Nouvelle-Aquitaine Council). Truc Vert monitoring site is labelled by the Service

Thème 6 – Risques côtiers

National d'Observation (SNO) Dynalit, with surveys further funded by Observatoire de la Côte de Nouvelle-Aquitaine (OCNA) and Observatoire Aquitain des Sciences de l'Univers (OASU).

8. References

- BERTSIMAS D., TSITSIKLIS J. (1993). *Simulated Annealing*. *Statistical Science*, 8(1), 10–15. <https://doi.org/10.1214/ss/1177011077>
- CASTELLE B., BUJAN S., MARIEU V., FERREIRA S. (2020). *16 years of topographic surveys of rip-channelled high-energy meso-macrotidal sandy beach*. *Scientific Data*, 7(1). <https://doi.org/10.1038/s41597-020-00750-5>
- CASTELLE B., MASSELINK G., SCOTT T., STOKES C., KONSTANTINOU A., MARIEU V., BUJAN S. (2021). *Satellite-derived shoreline detection at a high-energy meso-macrotidal beach*. *Geomorphology*, 383. <https://doi.org/10.1016/j.geomorph.2021.107707>
- DAVIDSON M.A., SPLINTER K.D., TURNER I.L. (2013). *A simple equilibrium model for predicting shoreline change*. *Coastal Engineering*, 73, 191–202. <https://doi.org/10.1016/j.coastaleng.2012.11.002>
- GALLAGHER E.L., MACMAHAN J., RENIERS A.J.H.M., BROWN J., THORNTON E.B. (2011). *Grain size variability on a rip-channelled beach*. *Marine Geology*, 287(1–4), 43–53. <https://doi.org/10.1016/j.margeo.2011.06.010>
- HERSBACH H., BELL B., BERRISFORD P., HIRAHARA S., HORANYI A., MUNOZ-SABATER J., NICOLAS J., PEUBEY C., RADU R., SCHEPERS D., SIMMONS A., SOC, C., ABDALLA S., ABELLAN X., BALSAMO G., BECHTOLD P., BIAVATI G., BIDLOT J., BONAVIDA M., THEPAUT J.N. (2020). *The ERA5 global reanalysis*. *Quarterly Journal of the Royal Meteorological Society*, 146(730), 1999–2049. <https://doi.org/10.1002/qj.3803>
- IBACETA R., SPLINTER K.D., HARLEY M.D., TURNER I.L. (2020). *Enhanced coastal shoreline modeling using an ensemble Kalman filter to include nonstationarity in future wave climates*. *Geophysical Research Letters*, 47(22). <https://doi.org/10.1029/2020GL090724>
- LARSON M., HOGAN L.X., HANSON H. (2010). *Direct formula to compute wave height and angle at incipient braking*. *Journal of Waterway Port, Coastal and Ocean Engineering* 136(2): 119-122. [https://doi.org/10.1061/\(ASCE\)WW.1943-5460.0000030](https://doi.org/10.1061/(ASCE)WW.1943-5460.0000030)
- SPLINTER K.D., TURNER I.L., DAVIDSON M.A., BARNARD P., CASTELLE B., OLTMAN-SHAY J. (2014). *A generalized equilibrium model for predicting daily to interannual shoreline response*. *Journal of Geophysical Research: Earth Surface*, 119(9), 1936–1958. <https://doi.org/10.1002/2014JF003106>
- VOS K., SPLINTER K.D., HARLEY M.D., SIMMONS J.A., TURNER I.L. (2019). *CoastSat: A Google Earth Engine-enabled Python toolkit to extract shorelines from publicly available satellite imagery*. *Environmental Modelling and Software*, 122. <https://doi.org/10.1016/j.envsoft.2019.104528>